

## Vorticity with varying collision energy in relativistic heavy ion collisions

Abhisek Saha<sup>1\*</sup> and Soma Sanyal<sup>2</sup>

<sup>1,2</sup>University of Hyderabad, Hyderabad - 500046, INDIA

### Introduction

We study the vorticity patterns in relativistic heavy ion collisions with respect to the collision energy. The collision energy is related to the chemical potential of the thermal - statistical models that assume chemical equilibrium after the relativistic collision. We use the multiphase transport model (AMPT) to study the vorticity. We look at the flow patterns related to the bulk viscosity and the shear viscosity at different collision energies. We find that the shear viscosity obtained is almost a constant with a small decrease at higher collision energies. We also look at the elliptic flow as it is related to viscous effects in the final stages after the collision.

### Vorticity simulation

We have used the AMPT code which is a multiphase transport model to generate the initial distribution of the particles [1]. The parameters that we use have been used previously in the AMPT model [2] to reproduce the yields, transverse momentum spectra, and elliptic flow for low- $p_T$  pions and kaons in central and midcentral  $Au + Au$  collisions at collision energies of 200 GeV. The output gives the particles space-time coordinates and three momentum at freeze-out. We then use a grid based simulation and obtain the average momentum and the energy for each cell. The velocity is extracted from these values by taking  $\frac{\langle \vec{p} \rangle}{\langle \epsilon \rangle}$ . We calculate the weighted vorticity on the XZ plane, both non-relativistic as well as relativistic with respect to the collision energy. In the reaction plane, the thermal vorticity is given by,  $\omega_{\mu\nu}^T = \frac{1}{2}(\partial_\nu \beta_\mu - \partial_\mu \beta_\nu)$ ,

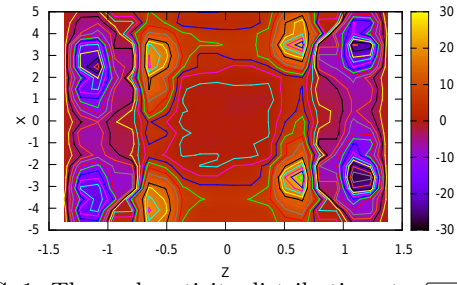


FIG. 1: Thermal vorticity distribution at  $\sqrt{s_{NN}}=200$  GeV for partons.

here  $\beta_\mu = \frac{u_\mu}{T}$ ,  $u_\mu = \gamma(1, -v_x, -v_y, -v_z)$  and  $T$  is the local temperature. Local vorticity depends on the velocity field at a particular instant and evolves as the velocity field evolves. In general, the bulk viscosity ( $\Pi$ ) is ignored and the shear viscosity ( $\eta$ ) is considered to be a constant. We use the definition of shear viscosity from Kadam et. al[3],  $\eta = \frac{5}{64\sqrt{8}r^2} \sum_i \langle |p| \rangle > \frac{n_i}{n}$ , here  $n_i$  is the number density of the  $i$  th particle while  $r$  is the radius of the particles concerned. At chemical equilibrium, the energy dependence of the baryon chemical potential is parametrized as,  $\mu_B(\sqrt{s}) = \frac{d}{(1+\epsilon\sqrt{s})}$ , ( $d = 1.308 \pm 0.028 GeV$ ,  $e = 0.273 \pm 0.008 GeV^{-1}$ )[4]. Hence chemical potential varies inversely as the collision energy.

### Results and Discussion

We have obtained the thermal vorticity patterns in the reaction (x-z) plane at an collision energy between 200 GeV and 20 GeV[5]. In fig 1, we see the vortex lines indicate distinct contours around the vortices formed. When we go lower in collision energy, the contours are far more spaced out. As the collision energy decreases, the chemical potential  $\mu_B$  increases. The vorticity formed tends to be circular if the angular momentum is higher and strain due

\*Electronic address: saha\_abhisek@yahoo.com

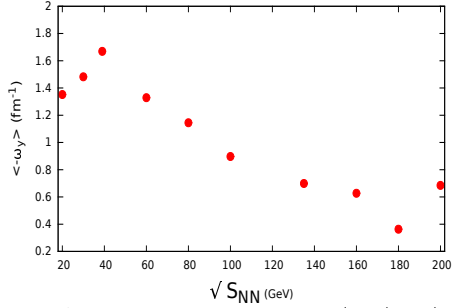


FIG. 2: Average thermal vorticity  $\langle \omega_{xz} \rangle \equiv \langle \omega_y \rangle$  at different  $\sqrt{s_{NN}}$  at an impact parameter  $b = 7fm$

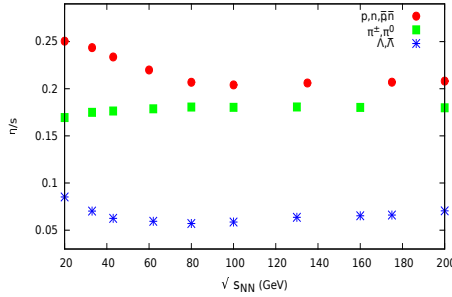


FIG. 3: The specific shear viscosity at different  $\sqrt{s_{NN}}$  for neutrons and protons, pions,  $\Lambda$  hyperons and their antiparticles.

to the bulk viscous pressure is lower. As the strain due to the bulk viscous pressure around the fluid increases, the vortices spread out and become more elliptical.

We studied the vorticities using the classical and relativistic definitions for the same energy range. In all the cases, we observe that the vorticity spreads out as we go to lower collision energies. The average thermal vorticity  $\langle \omega_{xz} \rangle$  is plotted at different collision energies in fig.2 and it shows that the average vorticity decreases with the increase in collision energy with a small dip below 40 GeV. Our vorticity results are consistent with ref.[6].

We obtain the coefficient of shear viscosity for various collision energies. Though defined over all the particles, we do the calculations separately over various particles specifically for neutrons, protons, pions and  $\Lambda$  hyperons as the number of these particles are greater in the output of the AMPT.

Fig.3 shows the viscosity of the neutrons, protons, pions and  $\Lambda$  hyperons. The specific shear viscosity is highest at lower collision

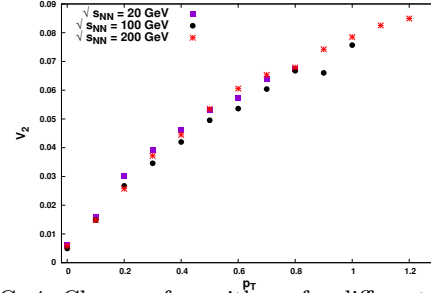


FIG. 4: Change of  $v_2$  with  $p_T$  for different  $\sqrt{s_{NN}}$  energies which corresponds to higher baryon chemical potentials. It becomes nearly constant beyond 80 GeV. Since vorticity diffuses through the viscous stresses. So the spreading out of the vorticity patterns indicate that the bulk pressure plays a greater role in the viscous diffusion of the vortices at low collision energies and high chemical potential. In fig.4, we show the nature of the elliptic flow changes with change in collision energy. At lower  $p_T$ , the different collision energies indicate that the overall  $p_T$  suppression is more for higher collision energies while no such conclusion can be reached for the higher  $p_T$  range. Even for 200 GeV we see that the  $v_2$  vs.  $p_T$  plot does not change significantly, when compared to the 20 GeV plot. So if shear viscosity indeed plays an important role in generating the elliptic flow, shear viscosity does not change significantly with increasing baryon chemical potential. This appears to agree with our plot of  $\frac{\eta}{s}$  vs  $\sqrt{s_{NN}}$ .

A.S is supported by INSPIRE Fellowship of the Department of Science and Technology, Govt. of India, ( Grant no: IF170627).

## References

- [1] Z. W. Lin et. al. Phys. Rev. C 72 064901 (2005).
- [2] Y. Jiang et. al., Phys. Rev. C 94, 044910 (2016).
- [3] G.P. Kadam and H. Mishra, Nucl. Phys. A 934, 133-147 (2015).
- [4] J. Cleymans, et.al., Phys.Rev.C 73: 034905,(2006).
- [5] A. Saha, S. Sanyal, arXiv:1902.08368v2 [hep-ph].
- [6] W.T. Deng et.al., Phys. Rev. C 93, 064907 (2016).